Cell

Coreceptor Scanning by the T Cell Receptor Provides a Mechanism for T Cell Tolerance

Ondrej Stepanek,[1,*] Arvind S. Prabhakar,[2] Celine Osswald,[1] Carolyn G. King,[1] Anna Bulek,[3] Dieter Naeher,[1] Marina Beaufils-Hugot,[1] Michael L. Abanto,[1] Virginie Galati,[1] Barbara Hausmann,[1] Rosemarie Lang,[1] David K. Cole,[3] Eric S. Huseby,[4] Andrew K. Sewell,[3] Arup K. Chakraborty,[2,5,6,7] and Ed Palmer[1,7,*]

[1]Departments of Biomedicine and Nephrology, University Hospital Basel and University of Basel, 4031 Basel, Switzerland
[2]Department of Chemical Engineering, Massachusetts Institute of Technology, Cambridge, MA 02139, USA
[3]Institute of Infection and Immunity, Cardiff University School of Medicine, Cardiff CF14 4XN, UK
[4]Department of Pathology, University of Massachusetts Medical School, Worcester, MA 01655, USA
[5]Institute for Medical Engineering and Science, Departments of Physics, Chemistry, and Biological Engineering, Massachusetts Institute of Technology, Cambridge, MA 02139, USA
[6]Ragon Institute of MGH, MIT, and Harvard, 400 Technology Square, Cambridge, MA 02139, USA
[7]Co-senior author
*Correspondence: ondrej.stepanek@unibas.ch (O.S.), ed.palmer@unibas.ch (E.P.)
http://dx.doi.org/10.1016/j.cell.2014.08.042

SUMMARY

In the thymus, high-affinity, self-reactive thymocytes are eliminated from the pool of developing T cells, generating central tolerance. Here, we investigate how developing T cells measure self-antigen affinity. We show that very few CD4 or CD8 coreceptor molecules are coupled with the signal-initiating kinase, Lck. To initiate signaling, an antigen-engaged T cell receptor (TCR) scans multiple coreceptor molecules to find one that is coupled to Lck; this is the first and rate-limiting step in a kinetic proofreading chain of events that eventually leads to TCR triggering and negative selection. MHCII-restricted TCRs require a shorter antigen dwell time (0.2 s) to initiate negative selection compared to MHCI-restricted TCRs (0.9 s) because more CD4 coreceptors are Lck-loaded compared to CD8. We generated a model (Lck come&stay/signal duration) that accurately predicts the observed differences in antigen dwell-time thresholds used by MHCI- and MHCII-restricted thymocytes to initiate negative selection and generate self-tolerance.

INTRODUCTION

T cells regulate adaptive immune responses to pathogens and tumors but can also drive autoimmune diseases. The T cell antigen receptor (TCR) on conventional αβT cells recognizes peptide fragments bound to class I or class II major histocompatibility complexes (pMHCI or pMHCII). Each developing T cell expresses a unique TCR and generation of a self-MHC restricted and self-tolerant T cell repertoire results from a multistep selection process in the thymus. Thymocytes expressing a TCR weakly reactive to the host's self-antigens receive a maturation signal to generate the functional T cell repertoire in the periphery (positive selection). In contrast, thymocytes with strongly self-reactive TCRs receive a death signal (negative selection). A failure to prevent strongly self-reactive T cells from entering the peripheral T cell pool is one of the main causes of autoimmune diseases (Yin et al., 2013). How thymocytes discriminate between positive- and negative-selecting antigens in the thymus is incompletely understood. Another open question is how a thymocyte balances the high sensitivity required to recognize just a few molecules of strong antigens (Ebert et al., 2008; Peterson et al., 1999) with the selectivity needed to discriminate between positive- and negative-selecting antigens even at relatively high densities (Daniels et al., 2006; Naeher et al., 2007).

Engagement of a TCR by its cognate ligand leads to phosphorylation of TCR-associated ITAM-containing TCRζ and CD3 chains by a Src family kinase, Lck (Straus and Weiss, 1992). Antigen discrimination might already occur at this step, because positive selecting antigens poorly induce phosphorylation of TCRζ chain (Kersh et al., 1998). Doubly phosphorylated ITAMs recruit ZAP70, a kinase that is subsequently activated by a second round of Lck-mediated phosphorylation (Straus and Weiss, 1993). ZAP70 relays the signal downstream by phosphorylating LAT and SLP76 (Smith-Garvin et al., 2009).

The CD4 and CD8 coreceptors bind to MHCII and MHCI, respectively. It has been suggested that the principal role of coreceptors is to enhance TCR signaling by delivering Lck to an engaged TCR (Artyomov et al., 2010; Veillette et al., 1988). CD8 additionally stabilizes TCR-pMHC interaction (Stone et al., 2009). Although signaling can be induced by very strong agonists or anti-TCR antibodies in the absence of coreceptors (van der Merwe and Dushek, 2011), CD4 or CD8 are required for signaling induced by most ligands (Kerry et al., 2003; Vidal et al., 1999). Moreover, coreceptors are vitally important for selecting T cells that recognize pMHCI and pMHCII antigens (Van Laethem et al., 2013). Along these lines, increasing Lck coupling

to CD8 enhances the efficiency of positive selection of MHCI-restricted thymocytes (Erman et al., 2006).

The strength of a self-antigen-TCR interaction dictates whether a developing thymocyte undergoes negative selection (Daniels et al., 2006; Hogquist et al., 1994; Williams et al., 1999). The main parameters describing the interaction between a TCR and its ligand are association rate (k_{on}), dissociation rate (k_{off}), and equilibrium dissociation constant (K_D). Whereas k_{off} determines the median dwell time of the antigen-TCR interaction ($\tau_{1/2} = \ln 2/k_{off}$), k_{on} (that is concentration-dependent) determines the rate of TCR-pMHC complex formation. K_D (= k_{off}/k_{on}) indicates the concentration-dependent occupancy of the TCR under equilibrium conditions. Although there are conflicting data whether k_{on}, k_{off}, K_D, or aggregate dwell time better describes the biological response induced by particular antigens, k_{off} predicts the magnitude of TCR responsiveness in most studies (Bridgeman et al., 2012; Govern et al., 2010; Huang et al., 2010; Kersh et al., 1998; Tian et al., 2007). Moreover, mathematical modeling and experiments with TCR-induced IFNγ production showed that biological potency correlated with an antigen's K_D, but that maximal response was determined by its k_{off} (Dushek et al., 2011).

T cells expressing a monoclonal TCR together with a set of altered peptide ligands (APL) are commonly used to address the issue of antigen discrimination by TCRs. OT-I is a murine TCR recognizing MHCI (H2-K^b) loaded with OVA peptide (SIINFEKL) or OVA-derived APLs. We previously showed that transgenic OT-I thymocytes discriminate between positive- and negative-selecting APLs in a manner that was largely dependent on antigen affinity and less dependent on a ligand concentration (Daniels et al., 2006). Two other MHCI-restricted TCRs could similarly discriminate between negative- and positive-selecting ligands. Threshold antigens were estimated to have on-cell K_D ~6 μM and $\tau_{1/2}$ ~1 s (Naeher et al., 2007; Palmer and Naeher, 2009). Moreover, negative, but not positive, selectors provoked a sufficiently strong response in mature CD8 OT-I T cells to induce autoimmunity in an experimental model of type I diabetes (King et al., 2012). These results indicate that T lineage cells sense an intrinsic binding parameter of their antigens. One plausible explanation includes the ability of a TCR to measure the duration of TCR-pMHC interactions (antigen dwell time), as suggested by a kinetic proofreading model of TCR triggering (McKeithan, 1995). However, the mechanism used by the TCR to sense antigen dwell time is largely unknown.

In this study, we show that an antigen-engaged TCR scans multiple coreceptors to find one that is coupled to Lck; this is the first and rate-limiting step in signal initiation. Based on experimental data and mathematical modeling, we propose a mechanism of TCR signaling (Lck come&stay/signal duration), where the kinetics of Lck delivery by coreceptors underlies a kinetic proofreading process that establishes a dwell-time threshold for negative selection.

RESULTS

Dwell-Time Threshold for Negative Selection by pMHCI versus pMHCII Ligands

To identify positive- and negative-selecting ligands for MHCII-restricted TCRs, we analyzed the development of I-A^b- restricted, peptide-specific B3K506 and B3K508 TCR transgenic Rag1$^{-/-}$ thymocytes exposed to a variety of APLs with known affinities (Huseby et al., 2005, 2006). Using the frequency of CD4 single positive (SP) cells as an indicator of negative selection in B3K508 fetal thymic organ cultures (FTOCs), we identified ligands behaving as negative selectors (3K, P5R, and P2A), one partial negative selector (threshold selector) (P-1A), and two ligands unable to negatively select (P3A, P-1K) (Figures 1A and 1B). Interestingly, negative- and positive-selecting ligands also affected the development of the CD8 SP compartment. Previous work showed that developing MHCII-restricted thymocytes undergoing negative selection generate a population of CD8αα innate-like T cells, while the same cells undergoing positive selection paradoxically select a minor population of CD8αβ SP cells (Yamagata et al., 2004). Similarly, in B3K508 FTOCs, only negative-selecting ligands generated a population of CD8αα SP cells, while CD8αβ SP thymocytes were present in FTOCs exposed to threshold and positive-selecting ligands (Figure S1A available online). Nevertheless, negative selection can be followed by the disappearance of the CD4 SP population. We also identified negative and threshold selectors using FTOCs from B3K506 Rag1$^{-/-}$ mice (Figure 1C). Threshold selectors for B3K508 and B3K506 thymocytes exhibited similar K_D values (263 μM and 319 μM, respectively) (Huseby et al., 2006), indicating that MHCII-restricted TCRs use a fixed affinity threshold (K_D ~300 μM) for negative selection.

To compare the affinities of threshold antigens mediating MHCI- and MHCII-restricted negative selection, we determined the affinities of several antigens for MHC-I restricted OT-I TCR using surface plasmon resonance (SPR) (Figures 1D and S1B–S1D). The threshold selector for OT-I thymocytes (K^b-T4) had a K_D value of 444 μM (Figure 1D) (Daniels et al., 2006). Taken together, results from our FTOC and SPR experiments argue that MHCI- and MHCII-restricted TCRs use a similar ligand affinity threshold to initiate negative selection. However, SPR affinity measurements neglect the roles of CD4 and CD8 coreceptors that bind to pMHCII and pMHCI antigens, respectively. Importantly, CD8, but not CD4, stabilizes the TCR-pMHC complex and prolongs a ligand's dwell time on the cell surface (Huppa et al., 2010; Naeher et al., 2007; Stone et al., 2009).

To directly determine the length of TCR-pMHC interactions in the presence of coreceptors, we measured the dwell times of Qdot-labeled-pMHC monomers on their respective peripheral T cells or double positive (DP) thymocytes by direct observation using single molecule microscopy (Movies S1 and S2). The observed dwell times could be fitted to a one-phase exponential decay curve (Figure 1E). For OT-I, an MHCI-restricted TCR, the $\tau_{1/2}$ of the various APLs on mature T cells range from 1 s to 16 s and the $\tau_{1/2}$ correlates well with antigenic potency (Daniels et al., 2006). The $\tau_{1/2}$ of the threshold selector, K^b-T4, is 1.3 s. Interestingly, the $\tau_{1/2}$s of strong negative selectors for the B3K506 (3K) and B3K508 (P1-A) MHCII-restricted TCRs are 1.3 s and 1.4 s, respectively.

We could not directly measure the dwell-time distribution of pMHCII threshold ligands, due to the speed of image acquisition. To estimate the $\tau_{1/2}$ for an MHCII-restricted threshold selector, we made some additional measurements.

We determined the $\tau_{1/2}$s of several ligands binding to their respective DP thymocytes (Figures 1E, panels 2 and 8, and

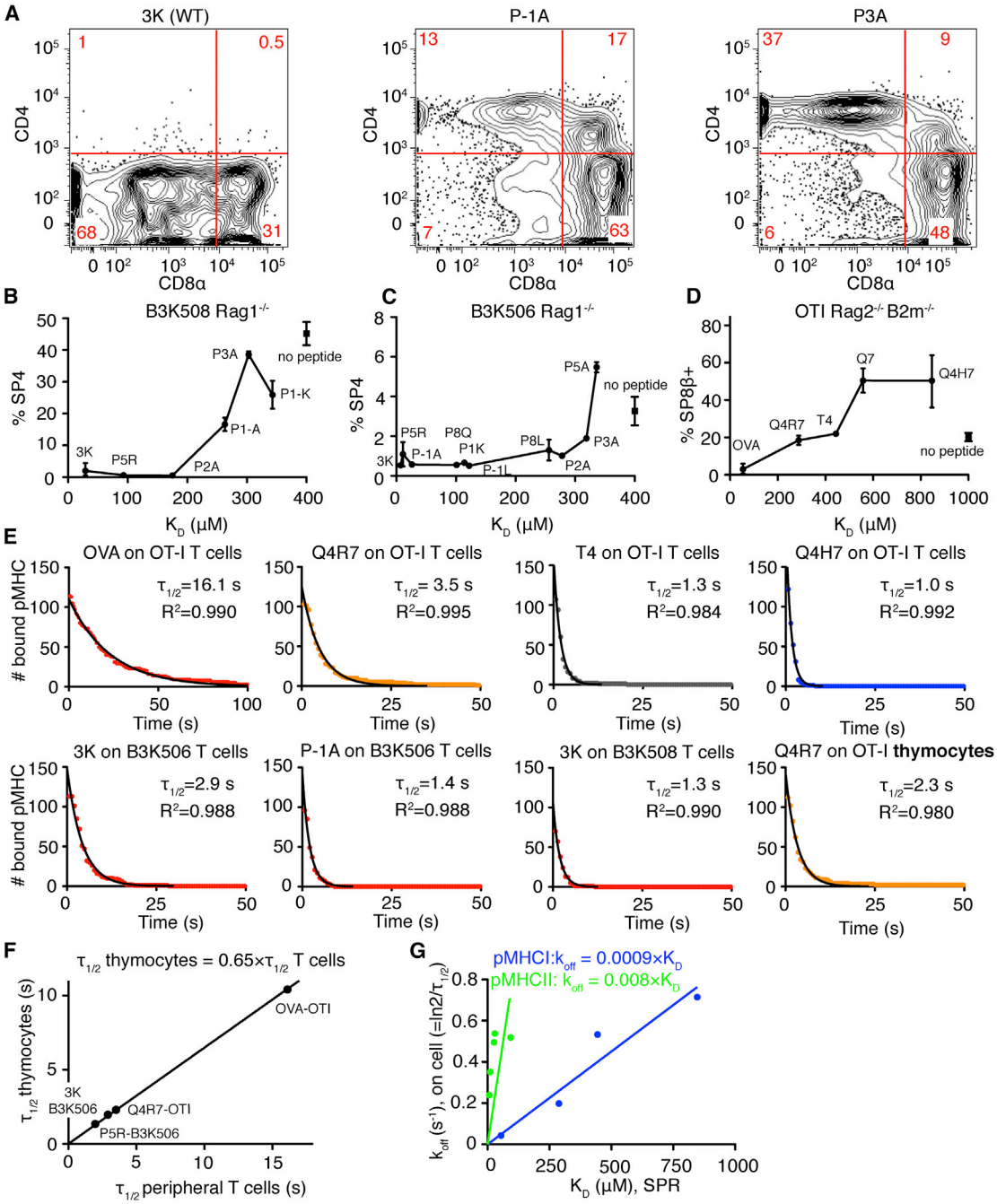

Figure 1. Thresholds for Negative Selection by pMHCII and pMHCI Ligands Show Similar SPR Affinities but Different On-Cell Dwell Times

(A–D) Fetal thymi from B3K508 Rag1$^{-/-}$ (A and B), B3K506 Rag1$^{-/-}$ (C), and OTI Rag2$^{-/-}$ β2 m$^{-/-}$ mice (D) were cultured with different APLs (20 μM) for 7 days and stained for CD4 and CD8. (A) Effects of 3K, P1-A, and P3A on the B3K508 Rag1$^{-/-}$ thymocyte development. Each panel is a representative plot from two thymi. (B–D) Percentage of CD4 or CD8β single positive cells versus K_D of APLs. Mean ± range, n = 2–5. Square symbol shows percentage of single positive cells without peptide (mean ± SEM, n = 5–11).

(E) Distribution of dwell times of pMHCI and pMHCII ligands on TCR transgenic CD4 or CD8 peripheral T cells, or preselection DP thymocytes. Data were fitted using one phase exponential decay curve.

(F) $\tau_{1/2}$ on preselection thymocytes versus $\tau_{1/2}$ on peripheral cells were plotted and fitted using linear regression with a fixed [0;0] point.

(G) k_{off}, calculated from on-cell $\tau_{1/2}$ on peripheral T cells versus K_D determined by SPR was plotted for pMHCI and pMHCII ligands and fitted with a linear regression with fixed [0;0] point.

See also Figure S1 and Table S1.

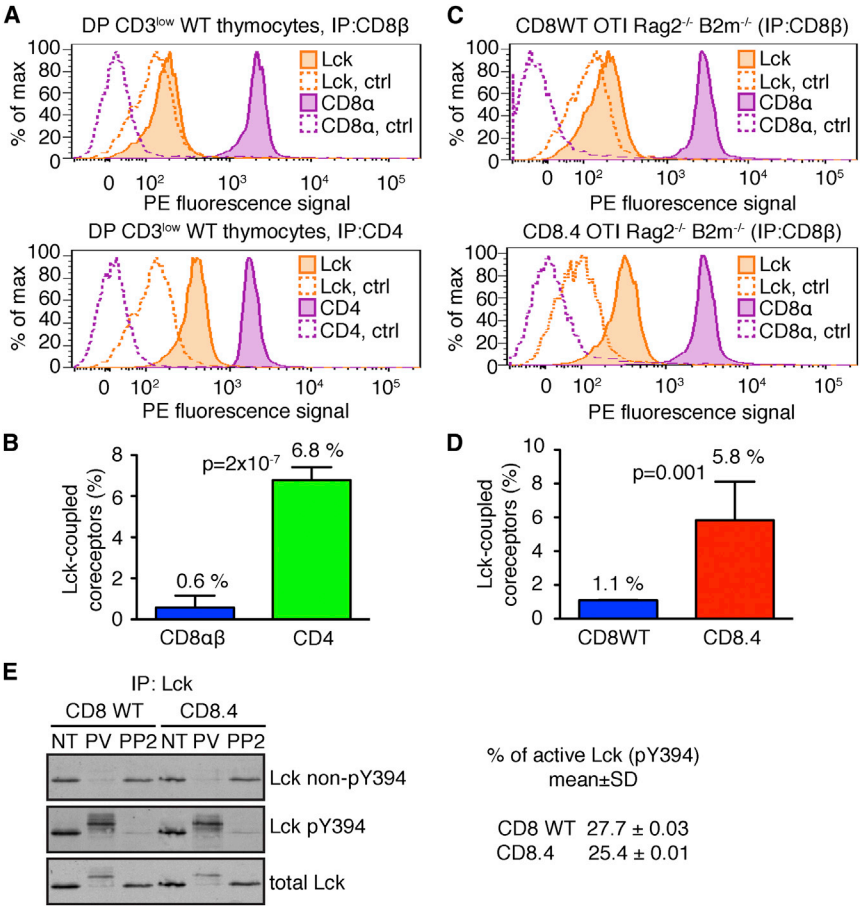

Figure 2. Quantitative Determination of Lck Coupling to CD4, CD8, and CD8.4 Coreceptors

Cell lysates were incubated with beads coated with antibodies to CD4, CD8β, or isotype controls. Beads were probed with PE-conjugated antibodies to Lck, CD8α, or CD4 and analyzed by flow cytometry.

(A–D) Sorted DP CD3low thymocytes from WT mice were analyzed (A and B). Thymocytes from CD8WT and CD8.4 OTI Rag2$^{-/-}$β2 m$^{-/-}$ mice were analyzed (C and D). Representative histograms (A and C) and aggregate data (B and D) (mean ± SD, n = 3–5) are shown. The p values were calculated using Student's t test (two-tailed, unequal variance). See also Figure S2.

(E) Lck was immunoprecipitated from lysates from nontreated (NT), pervanadate (PV), or 20 μM PP2-treated CD8WT and CD8.4 OTI Rag2$^{-/-}$ β2 m$^{-/-}$ thymocytes. Phosphorylation of Lck was analyzed by western blotting using simultaneous staining with Abs specific for phosphorylated or nonphosphorylated Y394. The membrane was reprobed with Ab to total Lck. Percentage of phosphorylated Lck molecules in resting CD8WT or CD8.4 DP thymocytes was calculated. CD8WT: n = 4; CD8.4: n = 5.

1F). The $\tau_{1/2}$s on DP thymocytes and peripheral T cells are in good agreement but the $\tau_{1/2}$s of a ligand binding to a thymocyte is approximately one-third shorter (Figure 1F). As peripheral T cells have substantially more TCR, the calculated $\tau_{1/2}$s on these cells may be slightly extended due to occasional rebinding to a second TCR. In any event, the threshold $\tau_{1/2}$s for negative selection of MHCI restricted thymocytes is ~0.9 s (Table S1).

We also observed that the on-cell k_{off} and SPR K_D are highly correlated, indicating that differences in K_D could be largely explained by differences in k_{off} (Figure 1G). Therefore, the extrapolated $\tau_{1/2}$ on thymocytes for pMHCII threshold antigens (K_D ~300 μM) is ~0.2 s (Table S1).

Thus, MHCI-restricted thymocytes use a longer dwell-time threshold for negative selection than MHCII-restricted thymocytes (0.9 versus 0.2 s). This raises the question, why MHCII-restricted thymocytes initiate negative selection with a shorter dwell time.

Extent of Coreceptor-Lck Coupling Determines the Threshold for Negative Selection

CD4 binds Lck better than CD8 (Wiest et al., 1993), which could explain the shorter dwell-time threshold for MHCII- versus MHCI-restricted thymocytes. We measured the CD4-Lck and CD8-Lck coupling ratios in polyclonal preselection DP thymocytes (B6) using immunoprecipitation followed by quantitative flow cytometric analysis (FC-IP). While only 0.6% of CD8αβ coreceptors bound Lck, 6.8% of CD4 molecules were Lck coupled (Figures 2A, 2B, and S2A). The CD4-Lck coupling in B3K508 and B3K506 preselection DP thymocytes was similar to that seen in polyclonal DPs from B6 mice (Figure S2B).

To further study the impact of coreceptor-Lck coupling on negative selection, we used homozygous CD8.4 knock-in mice (Erman et al., 2006), which are unable to express endogenous CD8α, and express instead only the chimeric CD8.4α chain, which consists of the extracellular part of CD8α and a cytoplasmic CD4 tail, which binds Lck. In OT-I DP thymocytes expressing CD8WT or CD8.4, coreceptor-Lck coupling is 1.1% and 5.8%, respectively (Figures 2C and 2D). It was important to know the percentage of coreceptors coupled with catalytically active Lck. For this reason, we used pair of antibodies recognizing active (pY394) and nonactive (non-pY394) Lck, respectively (Nika et al., 2010). This analysis indicated that the percentage of active Lck in the preselection DP thymocytes is 25%–28% (Figure 2E). Because the majority of Lck molecules are coreceptor-coupled (Van Laethem et al., 2007), the fraction of CD4 and CD8 coreceptors loaded with catalytically active Lck in DP thymocytes is 1.8% and 0.16%, respectively. Thus, the majority of coreceptors in DP thymocytes cannot initiate a TCR signal.

Expression of the CD8.4 coreceptor had no impact on the developmental arrest at the DP stage or surface TCR levels in the OT-I DP thymocytes (Figure S2C). Moreover, CD8.4 does not significantly affect antigen binding because K^b-Q4R7 binds to CD8WT and CD8.4 OT-I DP thymocytes with a similar $\tau_{1/2}$

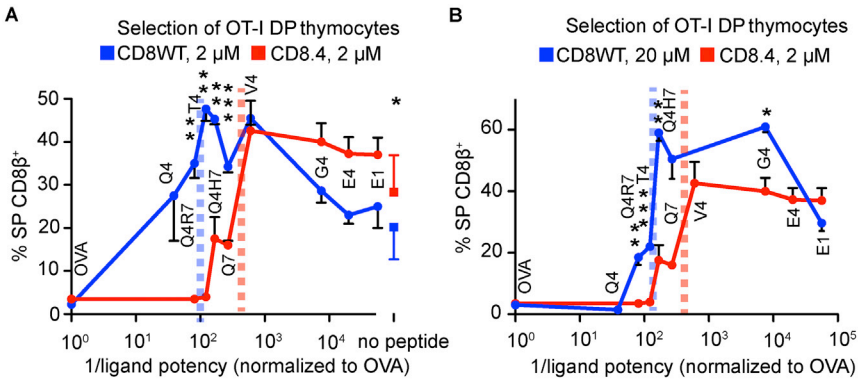

Figure 3. Enhanced Lck Coupling Lowers the Threshold for Negative Selection

Fetal thymi from CD8WT and CD8.4 OT-I Rag2$^{-/-}$β2 m$^{-/-}$ mice were exposed to OVA-derived APLs at the indicated concentrations Percentage of CD8β+ single positive cells versus 1/potency of the ligands (Daniels et al., 2006) is shown (mean ± SEM, n = 2–7). The squares show percentage of single positive cells generated with no peptide (mean ± SD, n = 11–12). The threshold for negative selection is marked by dashed vertical lines. Student's t test (two-tailed, unequal variance): *p < 0.05, **p < 0.01, *** < 0.001.
See also Table S1.

(Figures 1E and S2D). Despite these similarities, the threshold for negative selection was strikingly reduced in CD8.4 thymocytes, converting threshold and partial negative selectors (T4, Q4R7) into pure negative selectors and some positive selectors (Q4H7, Q7) into threshold selectors (Figure 3A). The effect of increasing CD8-Lck coupling cannot be mimicked by increasing the antigen concentration in CD8WT OT-I FTOCs (Figure 3B). Ten-fold higher concentrations (20 μM) of the APLs in CD8WT OT-I FTOCs do not generate the same degree of negative selection as 2 μM peptides used in CD8.4 OT-I FTOCs. Therefore, the increased Lck coupling to the CD8.4 coreceptor leads to a shorter dwell-time threshold for negative selection that is largely concentration insensitive. The impact of Lck-coupling on the development of thymocytes is summarized in Table S1.

Increased CD8-Lck Coupling Enhances Proximal Signaling and Cellular Responses

We further focused on the role of Lck coupling in the initiation of TCR signaling by analyzing the response of CD8WT and CD8.4 OT-I DP thymocytes to stimulation with various K^b-peptide tetramers (strong negative selector, K^b-OVA; just above threshold selector, K^b-Q4R7; positive selector, K^b-Q4H7). In CD8WT OT-I DP thymocytes, ligand-induced phosphorylation was modest for TCRζ and ZAP70 but downstream signaling proteins LAT, SLP76, VAV, and Erk1 exhibited more extensive phosphorylation upon stimulation (Figures 4A–4G and S3A–S3C). The data indicate an amplification step between ZAP70 activation and LAT phosphorylation. Importantly, CD8.4 thymocytes exhibited enhanced phosphorylation of TCRζ, ZAP70, LAT, SLP76, VAV, and Erk1 following TCR stimulation (Figures 4A–4G and S3A–S3C). The CD8.4 coreceptor increased overall TCR proximal signaling by 1.4, 3.7, and 5.8 following stimulation with K^b-OVA, K^b-Q4R7, and K^b-Q4H7, respectively (Figure S3D). Enhanced coreceptor-Lck coupling augments the proximal TCR signaling especially for lower affinity ligands.

Tetramer-stimulated CD8.4 thymocytes exhibited substantially increased calcium influx compared to CD8WT thymocytes (Figure 4H). In fact, CD8.4 thymocytes stimulated with below threshold K^b-Q4H7 tetramers exhibited a comparable level of calcium signaling as CD8WT thymocytes stimulated with high-affinity K^b-OVA tetramers, indicating a substantial shift in the signaling threshold induced by the chimeric coreceptor (compare purple and red curves in Figure 4H, upper left panel).

To address the role of CD8-Lck coupling in response to a broader range of APLs, CD8WT and CD8.4 OTI DP thymocytes were stimulated with antigen presenting cells (APCs) loaded with various peptide variants. We monitored induced expression of CD69, an activation marker that is upregulated both upon positive and negative selection (Figure S4). While CD8WT and CD8.4 thymocytes responded similarly to the strongest peptide, OVA, CD8.4 thymocytes were more sensitive to weaker antigens (Figures 5A–5C). The impact of enhanced Lck delivery mediated by the CD8.4 coreceptor inversely correlated with potency of the ligand (Figure 5D), consistent with the effects of CD8.4 on proximal signaling (Figure S3D).

Frequency of Coreceptor-Lck Coupling Determines the Kinetics of Lck Delivery to the TCR

The overall experimental data implied that Lck delivery is a limiting factor in signal initiation and potentially sets the dwell-time threshold to initiate negative selection. To better understand why coreceptor-Lck coupling is so important in this process, we generated a mathematical model that calculates the probability of recruiting an Lck-coupled coreceptor to an established TCR:pMHC pair as a function of time, when the CD4, CD8, or CD8.4 coreceptor is involved. The model is based on a Markov chain that describes the behavior of coreceptor and TCR-pMHC in the plasma membrane. A TCR-pMHC can form a pair (close proximity) or a complex (binding) with an empty or Lck-coupled coreceptor (Figure 6A). Because Lck-coupled coreceptors are relatively rare, a TCR-pMHC usually has to scan a large number of empty coreceptors before encountering an Lck-coupled one. The average time to recruit an Lck-loaded coreceptor to the TCR-pMHC is determined by the rate of coreceptor:TCR-pMHC complex formation, the duration of empty coreceptor:TCR-MHC interaction, and importantly, the percentage of Lck-coupled coreceptors (see Extended Experimental Procedures). The parameters used to construct the model were based on our measurements or published data (Figures S5A–S5C; Table S2). The model shows that Lck delivery is very fast in case of TCR-pMHCII interactions (CD4), but substantially slower upon TCR-pMHCI engagement (CD8). CD8.4 shows faster Lck recruitment than CD8WT (Figure 6B). When only active (pY394) Lck delivery is considered, the delivery of the Lck is delayed but the hierarchy of the coreceptors is maintained (dashed line in Figure 6B). Importantly, the model predicts that the probability of Lck recruitment is

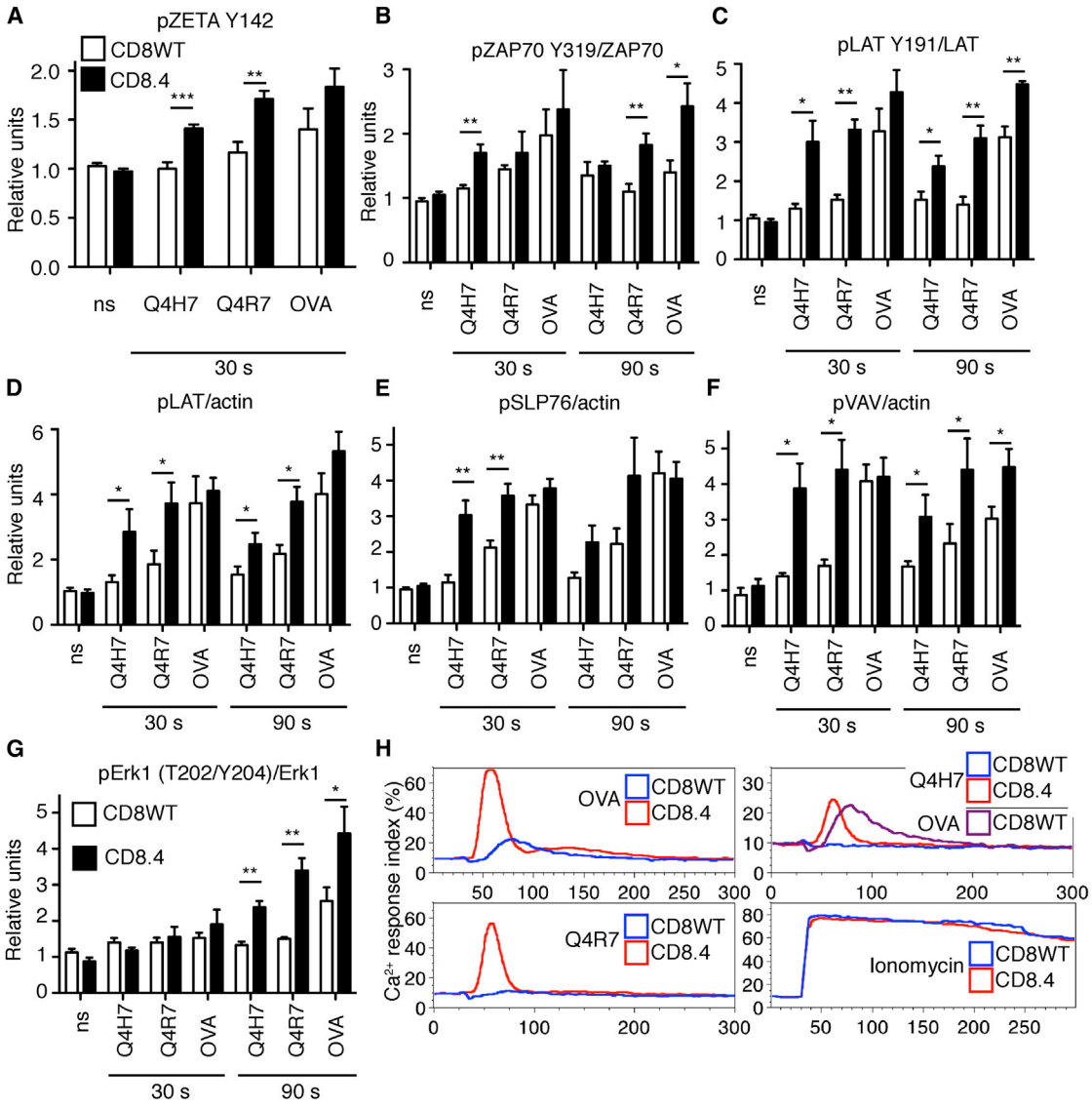

Figure 4. CD8.4 Enhances Proximal Signaling in OT-I Thymocytes

(A–G) Thymocytes from CD8WT or CD8.4 OT-I Rag2$^{-/-}$β2 m$^{-/-}$ mice were stimulated with 100 nM K^b-OVA, K^b-Q4R7, or K^b-Q4H7 tetramers or left unstimulated (ns). Results were normalized to the average of signal from unstimulated CD8WT or CD8.4 cells in each experiment. (A) Phosphorylation of TCRζ (Y142) was analyzed by flow cytometry on CD4+CD8+ population. Mean ± SEM, n = 6. (B, C, and G) Phosphorylation of LAT, ZAP70, and Erk was analyzed using phospho-specific Abs. Reprobing the membranes for total ZAP70, LAT, and Erk served as respective loading controls. (D–F) Phosphorylation of LAT, SLP76, and VAV in whole cell lysates was determined using anti-pTyr Ab and anti-actin Ab. as a loading control by western blotting. Mean ± SEM, n = 4. Statistical significance was tested using Student's t test (one-tailed, unequal variance): *p ≤ 0.05, **p < 0.01. See also Figure S3.

(H) CD8WT or CD8.4 OT-I DP thymocytes were loaded with Indo-1 and stimulated with 200 nM K^b-OVA, -Q4R7, or -Q4H7 tetramers or 1.5 μM ionomycine. Calcium mobilization was analyzed by flow cytometry. Ca^{2+} response index is shown (see Extended Experimental Procedures). A representative experiment from a total of three is shown.

highly dependent on the extent of coreceptor-Lck coupling (Figure 6C), underscoring its importance for setting the dwell-time threshold. Other parameters (number of CD8 molecules, diffusion coefficient of membrane anchored receptors, coreceptor-TCR interaction kinetics, and lattice spacing) play less important roles (Figure 6D).

To provide experimental evidence that a single TCR-pMHC complex serially engages large number of coreceptors, we carried out the following experiment. Qdot-labeled K^b-OVA or K^b-Q4R7 monomers were bound to OT-I DP thymocytes allowing the coengagement of the TCR and CD8 with the labeled antigen. After reaching equilibrium binding, the cells were diluted in presence or absence of an anti-CD8β mAb. Blocking the unengaged CD8 molecules accelerated the off-rate of pMHC dissociation (Figures S5E and S5F). This is consistent with the idea that during the life time of a pMHC-engaged TCR, there is significant

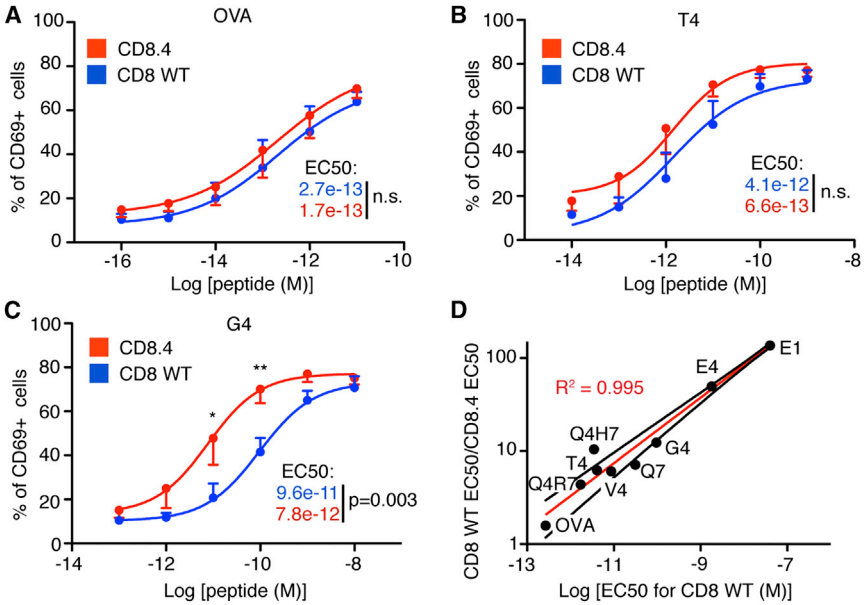

Figure 5. CD8.4 Preferentially Enhances Response to Weak Ligands

(A–C) Thymocytes from CD8WT and CD8.4 OT-I Rag2$^{-/-}$β2 m$^{-/-}$ mice were incubated with APCs loaded with varying concentrations of different peptides. After 24 hr, the percentage of CD69+ thymocytes was measured by flow cytometry. Response to OVA (A), T4 (B), and G4 (C) is shown. Mean ± SEM, n = 4. Statistical significance was tested using Student's t test (one-tailed, unequal variance): *p < 0.05, **p < 0.01.

(D) CD69 response of CD8WT and CD8.4 OT-I DP thymocytes to different antigens was examined and EC_{50} values were calculated. Ratio of EC_{50} CD8WT/EC_{50} CD8.4 was plotted versus EC_{50} CD8WT. Results show that CD8.4 thymocytes are preferentially more sensitive to weaker ligands, compared to CD8WT thymocytes. Red line shows the log-log line fit and the black lines represent 95% confidence intervals.

See also Figure S4.

turnover of CD8 molecules, which only transiently bind to the pMHC. This coreceptor exchange would allow the engaged TCR to eventually find an Lck coupled coreceptor if the pMHC engagement is sufficiently long.

Lck Delivery Is the Initial Step during Kinetic Proofreading

The Markov chain model explained the importance of the proportion of Lck-coupled coreceptors and coreceptor exchange in determining the speed of the signal initiation. We subsequently generated four different models that extended the Markov chain model by combining Lck delivery together with its kinase activity. Comparison of the models' predictions with the experimental data should indicate the actual molecular mechanism that initiates TCR triggering and sets the antigen dwell-time threshold for negative selection.

For all four models, we assumed that the recruited Lck has to minimally phosphorylate four tyrosines (two ITAM tyrosines and Y315 and Y319 in ZAP70) to obtain ZAP70 activation and signal propagation. The actual number of tyrosine phosphorylations is likely higher because phosphatase activity can counteract the Lck activity and Lck might phosphorylate tyrosines in separate ITAMs. Thus, we set five phosphorylations by an Lck molecule as a criterion for TCR triggering to make it more than the minimal number.

Our preferred model, "Lck come&stay/signal duration," combines the Lck recruitment calculated from the Markov chain model with the classical TCR kinetic proofreading model (McKeithan, 1995). In this model, we assumed the following scenario. A newly formed TCR-pMHC pair eventually interacts with a coreceptor coupled to active Lck (pLck). The coreceptor-pLck remains attached to the TCR-pMHC complex due to the interactions of Lck's SH2 domains with partially phosphorylated TCR (and/or ZAP70) and stabilization via the pMHC:coreceptor interaction (Jiang et al., 2011; Straus et al., 1996). Lck triggers TCR signaling by phosphorylating ITAM tyrosines and a subsequently recruited ZAP70. Active ZAP70 continuously generates downstream signals by phosphorylating LAT, SPL76, and other signaling molecules. When antigen disengages from the TCR, coreceptor-Lck is released as well, leading to a massive decrease in kinase activity. This shifts the kinase/phosphatase equilibrium toward phosphatase activity and sets the TCR and ZAP-70 back into a less phosphorylated state. "'Lck come&stay/signal duration" model assumes that the TCR-pMHC interaction has to last long enough to recruit and activate ZAP70. Once the ZAP70 is activated, further antigen occupancy of the already triggered TCR determines the strength of the TCR signal. The overall TCR signal induced in a thymocyte is determined by the number of triggered TCRs and the amount of time they remain occupied by pMHC subsequent to TCR triggering (Extended Experimental Procedures; Table S3). The model calculates total TCR signal as a function of number of antigen molecules available in the thymocyte/APC interface and their $\tau_{1/2}$ (Figures 7A and S6A). In contrast to a pure TCR occupancy model (Figure 7B) that predicts little discrimination between ligands with different dwell times, the "Lck come&stay/signal duration" model displays the kinetic proofreading principle. Our data clearly show that antigens with $\tau_{1/2}$ ~10 s (K^b-OVA) can negatively select at low concentrations; antigens with $\tau_{1/2}$ ~1–2 s (Kb-T4 and Kb-Q4R7) negatively select at higher concentrations; and antigens with $\tau_{1/2} \leq 0.6$ s (Kb-Q4H7) are incapable of negative selection even when present at very high concentrations in the synapse (i.e., 250 cognate pMHC, which is ~5%–10% of the pMHCI pool at the interface). The model assumes that as few as two to four triggered and occupied TCRs can initiate negative selection, which has previous experimental support (Ebert et al., 2008; Peterson et al., 1999).

The model predicts a shift of the dwell-time threshold for negative selection in CD8.4 cells (Figures 7A and 7C), which in good agreement with the experimental data (Figures 1 and 3; Table S1). Moreover, this model predicts that the shorter the $\tau_{1/2}$ of a TCR ligand is, the more pronounced is the difference between

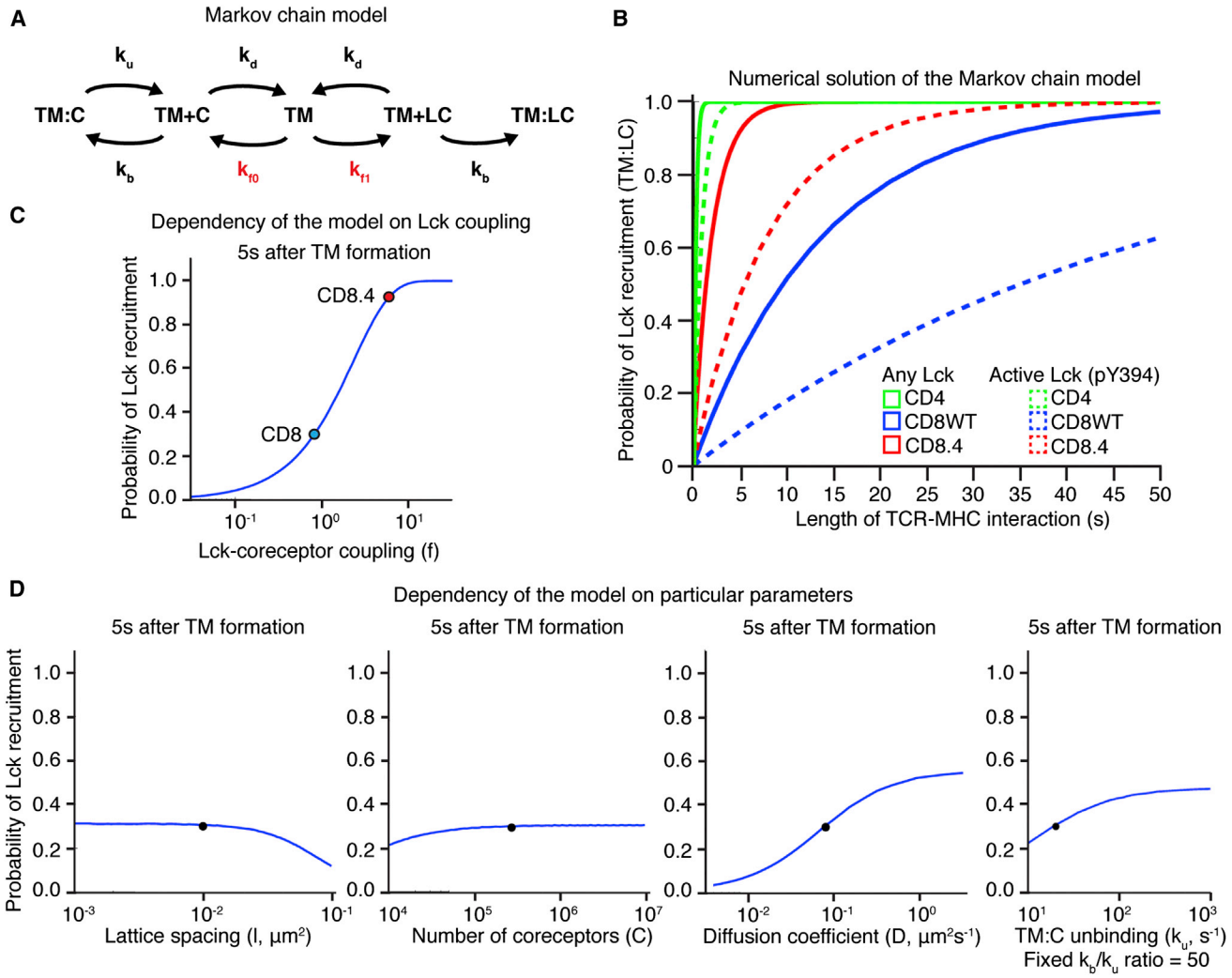

Figure 6. Markov Chain Model for Lck Delivery to the TCR-pMHC Pair

(A) Scheme of the Markov chain model describing kinetics of protein interactions in the plasma membrane. TM is a TCR-pMHC pair, C is an empty coreceptor, and LC is an Lck coupled coreceptor. TM+C and TM+LC represent coreceptor and TCR-pMHC pairs (in close proximity), TM:C and TM:LC represent coreceptor-TCR-pMHC complexes (binding). The complex of Lck-coupled coreceptor and TCR-pMHC (TM:LC) is an absorbing end state. K_D, k_b, k_u, k_{f0}, k_{f1} represent kinetic rates (Table S2). The rates that depend on the extent of coreceptor-Lck coupling are shown in red.

(B) Numerical solution of Markov chain model. The probability of TM:LC complex formation as a function of time was calculated for CD4 (pMHCII), CD8WT (pMHCI), and CD8.4 (pMHCI). Both the probability of recruitment of any Lck-coupled coreceptor (solid line) or a coreceptor coupled to active Lck (pY394) is shown (dashed line).

(C) Probability of TM:LC pair formation as a function of CD8-Lck coupling for MHCI ligand. The values for CD8WT (blue dot) and CD8.4 (red dot) are marked. Other parameters remained fixed.

(D) The probabilities of TM:LC formation as a function of lattice spacing, coreceptors number, CD8 and TCR diffusion coefficient and CD8:MHC unbinding k_u (when k_u/k_b ratio was fixed) for MHCI ligand and CD8 coreceptor. The original parameters are marked (black dot).

See also Extended Experimental Procedures, Figure S5, and Table S2.

CD8.4 and CD8WT signaling (Figure 7D). This is essentially in agreement with the experimental data (Figures 4 and 5). The "Lck come&stay/signal duration" model predicts the dwell-time thresholds used by polyclonal pMHCI- and pMHCII-restricted thymocytes (~1 s for MHCI and ~0.2 for MHCII antigens) (Figure 7E). The model also reveals that antigens with $\tau_{1/2}$ at or just above the dwell-time threshold must be presented at a relatively high copy number to induce negative selection (e.g., 50 molecules of pMHCI antigens with $\tau_{1/2}$ ~2 s). If such peri-threshold ligands are presented at low numbers in the thymus, but at higher levels in peripheral tissues, the generation of central self-tolerance may be defective.

The serial triggering (productive hit) model assumes that once a TCR is triggered, continued pMHC binding does not further increase the TCR signal (Dushek et al., 2011; Valitutti, 2012). We also constructed a combined "Lck come&stay/serial triggering" model that assumes that the total TCR signal is determined by the number of triggered TCRs. However, the "Lck

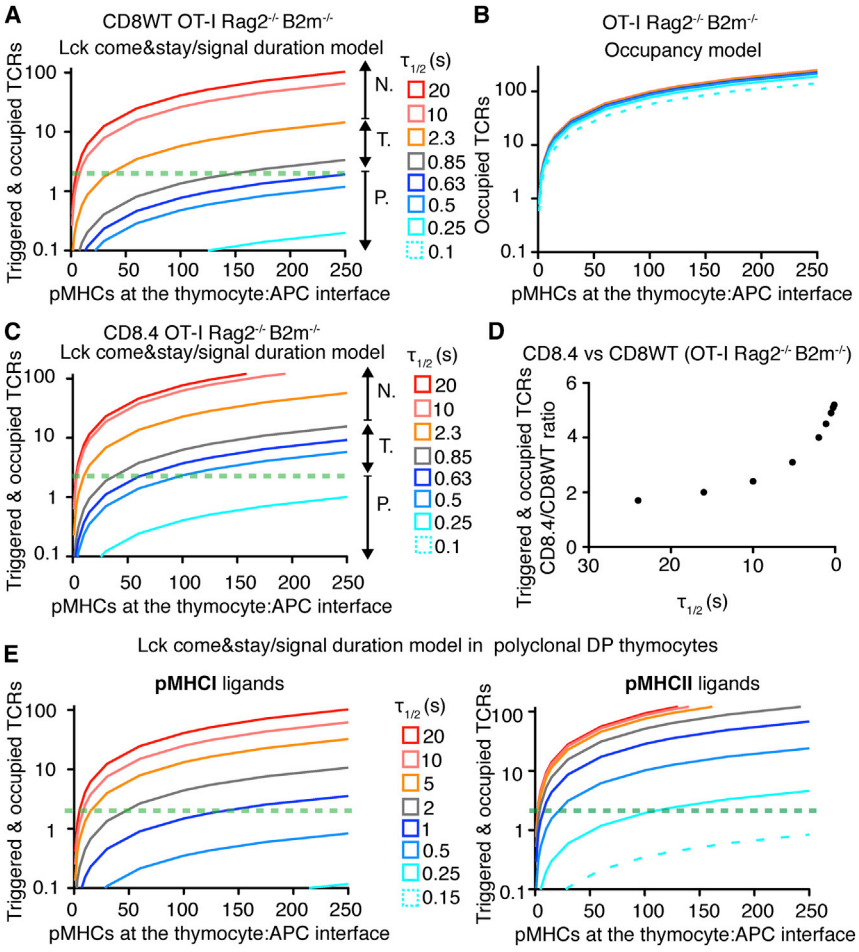

Figure 7. Model of Lck Recruitment Combined with Kinetic Proofreading Predicts Experimental Data

Graphs show TCR signal intensity as a function of number of cognate ligands at the thymocyte/APC interface for different ligands (k_{on} = 0.1 $\mu m^2 s^{-1}$, $\tau_{1/2}$ variable). Horizontal green dashed line shows the likely threshold when two TCRs are triggered and still occupied.

(A) "Lck come&stay/signal duration" model for CD8WT OT-I Rag2$^{-/-}$ β2 m$^{-/-}$ thymocytes. N, negative selectors; T, threshold ligands (partial negative selectors); P, positive selectors.

(B) Pure TCR occupancy model for OT-I Rag2$^{-/-}$ β2 m$^{-/-}$ thymocytes.

(C) "Lck come&stay/signal duration" model for CD8.4 OT-I Rag2$^{-/-}$ β2 m$^{-/-}$ thymocytes.

(D) Difference between CD8.4- and CD8WT-mediated TCR signaling (CD8.4/CD8WT ratio) in OT-I Rag2$^{-/-}$ β2 m$^{-/-}$ thymocytes versus $\tau_{1/2}$ of a TCR ligand, predicted by the "Lck come&stay/signal duration" model. Advantage of increased Lck coupling (CD8.4) is increasingly apparent at low $\tau_{1/2}$.

(E) Comparison of TCR responses induced by pMHCI and pMHCII ligands in polyclonal preselection DP thymocytes predicted by the Lck come&stay/signal duration model.

See also Extended Experimental Procedures, Figure S6, and Table S3.

come&stay/serial triggering" model does not predict the experimentally observed hierarchy of the ligands, arguing that serial triggering cannot explain the negative selection threshold (Figure S6B).

We also generated two additional models requiring multiple visits of Lck to trigger the TCR (Figure S6C). In these models, we assumed that Lck is not stabilized at the TCR-pMHC and phosphorylates only one tyrosine upon a single interaction between a coreceptor-Lck molecule and the TCR-pMHC. Thus, coreceptor-Lck has to be repeatedly recruited to the TCR-pMHC to trigger the TCR. These models predict very strong discrimination between ligands based on their $\tau_{1/2}$, but displays very low sensitivity to ligands, just over the dwell-time threshold; this is not compatible with our experimental data. Given the poor predictive power of these last three models, the "Lck come&stay/signal duration" model clearly provides the best explanation of our experimental data.

DISCUSSION

Here, we describe a mechanism that allows thymocytes to discriminate antigens of differing median dwell times and establish an antigen dwell-time threshold for negative selection. During the time that a TCR binds a pMHC antigen, the TCR-pMHC complex scans up to several hundreds of coreceptors to find one, which carries catalytically active Lck; subsequently this recruited kinase phosphorylates ITAMs and activating tyrosines on ZAP70. Finding an Lck-loaded coreceptor represents the first and rate-limiting step in signal initiation, because only a minority of coreceptor molecules are actually coupled to active Lck. MHCI-restricted TCRs require antigens with a $\tau_{1/2}$ >0.9 s to induce negative selection, while the negative selection threshold for MHCII-restricted TCRs is $\tau_{1/2}$ >0.2 s. A higher frequency of CD4 molecules are coupled to catalytically active Lck compared to CD8 (2% versus 0.2%); for this reason, MHCII-restricted receptors have a shorter dwell-time threshold.

Modeling studies revealed that the frequency of Lck-coupled coreceptors is a critical parameter in establishing the dwell-time threshold for negative selection. The decrease in the dwell-time threshold for negative selection seen in CD8.4 OT-I mice is a consequence of CD8.4's increased coupling to Lck, resulting in a faster arrival of a coreceptor-pLck complex to an antigen-occupied TCR. CD8.4 mediates an enhanced activation of proximal TCR signaling pathways and, similar to CD4, allows negative selection by antigens with short dwell times. It is not clear whether having a shorter dwell-time threshold for the deletion of MHCII-restricted thymocytes provides an intrinsic advantage or whether this is simply a consequence of the differences in Lck coupling exhibited by CD4 and CD8. Nevertheless, these differences illustrate the mechanism, where the dwell-time threshold is set by the median time required for the antigen engaged TCR to find an Lck-loaded coreceptor.

To directly estimate the dwell-time threshold, we attached monomeric pMHCs to Qdots and observed the binding of monomeric pMHC to antigen-specific T cells by single molecule microscopy. The $\tau_{1/2}$ for the OT-I threshold ligand (K^b-T4) was estimated to 0.9 s on thymocytes and 1.3 s on peripheral T cells, which corresponds well to the dwell-time threshold for H2-K^d-restricted T1 TCR (0.8–1.5 s), estimated by an on-cell photoaffinity labeling technique (Naeher et al., 2007; Palmer and Naeher, 2009). How well does $\tau_{1/2}$ measured with soluble ligand (3D) correspond to antigen binding at the thymocyte/APC interface? Although the $\tau_{1/2}$ was originally viewed as a biophysical parameter describing ligand-receptor interactions independent of their spatial context (Dustin et al., 2001), several studies report that k_{off} is accelerated in a planar configuration (2D) of T cell-APC contacts (Huang et al., 2010; Huppa et al., 2010). However, other studies showed that pMHC $\tau_{1/2}$ measured using 2D or 3D techniques are similar, consistent with the original view (O'Donoghue et al., 2013; Robert et al., 2012). Recently, pMHCI/TCR dwell times were analyzed under tensile force in a 2D setting (Liu et al., 2014). Interestingly, TCR interactions with potent ligands are stabilized when a moderate force (5–10 pN) is applied due to the formation of catch bonds. The authors suggest that a tensile force generated at the thymocyte/APC interface contribute to TCR specificity. However, their results show that both positive and negative selectors can form catch bonds, so the formation of a catch bond per se does not explain the negative selection threshold. Nevertheless, the catch bond phenomenon can be easily integrated with our "Lck come&stay/signal duration model" that provides the signaling mechanism underlying TCR triggering and discrimination between negative and positive ligands based on their dwell times.

Interestingly, $\tau_{1/2}$ measurements in their system corresponded well with our on-cell measurements. We determined that the $\tau_{1/2}$ of OT-I:K^b-OVA is ~10 s, while Zhu and coworkers (Liu et al. 2014) measured the $\tau_{1/2}$ for the same antigen as 0.8 s under 10 pN; the ~10-fold difference is expected because of the absence of CD8 engagement in their system (Naeher et al., 2007). However, it remains unclear why an application of a moderate tensile force is required in the 2D setting, but not in our on-cell 3D assay, to measure biologically relevant dwell times of TCR-antigen interactions.

We generated four mathematical models describing TCR signaling response in thymocytes, using a combination of our measurements and published data as input parameters. The k_{on} (Huppa et al., 2010) was sufficiently high that it hardly limited the formation of TCR-pMHC bonds in the thymocyte:APC contact area. Ligand concentration and $\tau_{1/2}$ had the largest impact on the quantity of TCR signals generated. To find the most relevant model, we compared the outcome of the models with our experimental data on TCR signaling in CD8WT and CD8.4 OT-I DP thymocytes. The "Lck come&stay/Signal duration" model, which best explains our experimental data, is based on the principle of kinetic proofreading (McKeithan, 1995), where Lck recruitment is the most proximal limiting step. The model assumes that transient CD4-MHCII or CD8-MHCI interactions allow the TCR-pMHC pair to scan multiple coreceptors via coreceptor exchange before finding a coreceptor carrying catalytically active Lck. Nika et al. (2010) demonstrated that 38% of Lck molecules are catalytically active in human CD4+ T cells and moreover Lck does not undergo further activation upon TCR stimulation. Murine preselection DP thymocytes have a slightly lower percentage of active Lck (25%–28%), implying that only ~0.16% of CD8 and ~1.8% of CD4 molecules are capable of initiating a TCR signal. Following the recruitment of catalytically active Lck, the kinase phosphorylates ITAM tyrosines in the CD3 complex and subsequently phosphorylates a recruited ZAP70 kinase. Coreceptor-Lck binding to TCR-pMHC is potentially stabilized via an interaction of Lck's SH2 domain with a phosphotyrosine in an ITAM or ZAP70 (Jiang et al., 2011; Straus et al., 1996). If the TCR-pMHC interaction lasts long enough to enable Lck-mediated phosphorylation of ZAP70, then ZAP70 generates downstream signals by phosphorylating LAT and SLP76 for the duration of the TCR-pMHC interaction. The longer the duration of antigen binding, the more downstream mediators are generated. Signaling is terminated when the pMHC and subsequently, the coreceptor-Lck disengage from TCR. A thymocyte surveys a single APC for several minutes (Ebert et al., 2008; Melichar et al., 2013); over this time span, the decision to initiate negative selection must be made.

We propose that positive- and negative-selecting ligands induce quantitatively different responses at the level of TCR activation (i.e., number of TCRs kept triggered) that is transformed to qualitatively different events in downstream signaling pathways. Our model is in line with the observation that positive- and negative-selecting ligands induce distinct patterns of Erk activation (Daniels et al., 2006). Previous mathematical modeling suggested that only negative-selecting ligands are able to induce extensive LAT phosphorylation and trigger a feed-forward loop resulting in the activation of SOS and activation of pErk at the plasma membrane (Prasad et al., 2009).

The TCR has the unusual property of being able to recognize antigens with a high degree of sensitivity and an ability to discriminate between closely related structural variants. As few as two to four strong ligands within the thymocyte-APC contact area are able to trigger a strong TCR response and induce negative selection (Ebert et al., 2008; Peterson et al., 1999). This sensitivity has been explained by the ability of one pMHC ligand to trigger several TCRs and amplify the signal. However, evidence for serial triggering is so far indirect (Valitutti, 2012). Moreover, a strict serial triggering model does not explain our experimental data, because it predicts that threshold ligands (K^b-T4) will engage and trigger similar number of TCRs as long dwelling ligands (K^b-OVA). Furthermore, serial triggering could not be detected during direct observation of TCR-pMHC interactions in situ (O'Donoghue et al., 2013). Along this line, we propose that very few strong ligands are able to keep a few TCRs continually engaged and triggered; this amplifies the TCR signal by continuous generation of intracellular signaling intermediates. Higher numbers of less potent, but above threshold ligands are required to induce the same effect, while below threshold ligands are essentially unable to trigger negative selection.

The two models, which employ the Lck multiple visit assumption, are relatively insensitive. These models predict that only antigens with very long dwell times or present at high concentrations can initiate a TCR signal. For this reason, we do not favor these models. We also observed that the serial triggering

strategy poorly discriminates between antigens with differing median dwell times. On the other hand, the signal duration mechanism allows the amount of TCR generated signal to reflect the actual dwell time. Thus, the "Lck come and stay/signal duration" mechanism allows for antigen recognition, which is both highly sensitive and discriminatory.

"Lck come and stay/signal duration" model uncovers molecular events constituting for a TCR kinetic proofreading mechanism. Highly specific recognition of negative-selecting ligands by a developing thymocyte is an analogy to a kinetic proofreading that provides specificity in DNA, protein, and amino acid-tRNA synthesis (Hopfield, 1974). These diverse molecular processes have a built in time delay between a substrate binding the enzyme and its conversion into a product molecule. A substrate molecule (nucleotide, amino acid, etc.) that binds the respective enzyme for a longer time is more likely to be the biologically "correct" molecular species. The TCR and coreceptor operate under a similar principle; a long-lasting antigen binding event is more likely to be converted into a (negative selection) signaling event.

Our experimental results and mathematical models explain how the TCR actually measures antigen affinity to initiate a negative selection signal. The kinetics of Lck delivery by coreceptors plays a crucial role in setting the antigen dwell-time threshold for negative selection. The kinetic proofreading mechanism suggested by our model implies that collisions between hundreds of coreceptor molecules and a small number of antigen bound TCRs allow the developing thymocyte to sense the antigen's median dwell time and initiate a critical cell fate decision (negative selection).

EXPERIMENTAL PROCEDURES

Mice

All adult mice were 6–12 weeks old and had a C57Bl/6 genetic background. OT-I Rag2$^{-/-}$, OT-I Rag2$^{-/-}$ β2 m$^{-/-}$, B3K508 Rag1$^{-/-}$, and B3K506 Rag1$^{-/-}$ mice were described previously (Daniels et al., 2006; Huseby et al., 2005).

CD8.4 OT-I Rag2$^{-/-}$ β2 m $^{-/-}$ strain was generated by crossing CD8.4 knock-in mouse (Erman et al., 2006) with OT-I Rag2$^{-/-}$ β2 m$^{-/-}$. Mice were bred in our colony (University Hospital Basel) in accordance with Cantonal and Federal laws of Switzerland. Animal protocols were approved by the Cantonal Veterinary Office of Baselstadt, Switzerland.

Surface Plasmon Resonance

SPR equilibrium binding analysis was performed using a BIAcore T100™ equipped with a CM5 sensor chip. SPR equilibrium analyses were carried out to determine the K_D values for OT-I:H2-K^b-APL interactions at 25°C. Approximately 300 response units of pMHC or TCR were coupled to the CM5 sensor chip surface. Analyte was injected at concentrations ranging from ten times above and ten times below the estimated K_D of the interaction.

Flow Cytometry

Live cells were stained with relevant Abs on ice. For intracellular staining, cells were fixed in 4% paraformaldehyde (15 min, room temperature [RT]), permeabilized by 90% methanol (30 min, on ice) and stained with indicated antibodies at RT. Determination of surface molecule number was performed using saturating concentrations of PE-conjugated Abs and calibration beads. Calcium mobilization was measured using Indo-1 probe and Calcium response index was calculated (see Extended Experimental Procedures).

Flow cytometry immunoprecipitation (FC-IP) was done as described previously (Schrum et al., 2007). Briefly, beads coated with anti-CD4 or anti-CD8α Abs were used to pull down CD4 or CD8. Subsequently, PE-conjugated anti-CD4, anti-CD8β, or anti-Lck Abs were used to quantify Lck/CD8 and Lck/CD4 coupling ratios.

Flow cytometry was carried out with a FACSCantoII (BD Bioscience). Cell sorting was performed using an Influx sorter (BD Bioscience). Data were analyzed using FlowJo software (TreeStar).

Determination of Lck Phosphorylation Status

Lck was immunoprecipitated from untreated, or PV- or PP2-treated thymocytes and analyzed by western blotting. Signals from Abs recognizing phosphorylated and nonphosphorylated Lck (Y394) were normalized to total Lck and the percentage of phosphorylated molecules was calculated as previously described (Stepanek et al., 2011).

On-Cell Dwell-Time Measurement

Qdot-pMHC monomers were added to T cells or thymocytes attached to poly-lysine-coated borosilicate glass. Binding of Qdot-pMHC monomers was observed using single molecule microscopy for 2.5 min and the duration of pMHC binding events was measured. The number of persisting binding events was plotted versus time and fitted with to a one phase exponential decay function. See also Extended Experimental Procedures.

FTOC

FTOCs were performed as described (Hogquist et al., 1994). Briefly, thymic lobes were excised from mice at a gestational age of day 15.5 and incubated in the presence of particular peptide and, in case of OT-I Rag2$^{-/-}$ β2 m$^{-/-}$ thymi, exogenous β2 m (5 μg/ml). After 7 days of culture, thymocytes were analyzed by flow cytometry.

Western Blotting

Samples for western blotting were heated in Laemmli sample buffer (2 min, 95°C), sonicated and analyzed by SDS-PAGE and western blotting, using AlexaFluor790- or AlexaFluor680-conjugated goat anti-mouse or anti-rabbit secondary antibodies (Jackson ImmunoResearch). Specific Ab signals were quantified using an Odyssey Infrared Imaging System (LI-COR Biosciences) and analyzed by ImageJ software (NIH).

Mathematical Model

The models are composites of Markov chain model describing behavior of surface molecules, equations describing TCR occupancy, and equations describing initial catalytic steps in TCR triggering. The models predict either a number of triggered TCRs within a time interval or a number of occupied and triggered TCRs in any given time point.

SUPPLEMENTAL INFORMATION

Supplemental Information includes Extended Experimental Procedures, six figures, three tables, and two movies and can be found with this article online at http://dx.doi.org/10.1016/j.cell.2014.08.042.

AUTHOR CONTRIBUTIONS

O.S., C.O., C.G.K., M.L.A., M.B., D.K.C., A.K.S., D.N., and E.P. designed experiments. O.S., C.G.K., C.O., M.L.A., B.H., V.G., M.B., A.B., D.K.C., A.K.S, E.P., D.N., and R.L. performed experiments and analyzed data. O.S., A.S.P., and A.K.C. generated the mathematical models. E.S.H. provided mice and generated MHCII monomers. O.S. and E.P. wrote the manuscript. All authors commented on the manuscript draft. A.K.C., E.S.H., A.K.S., and E.P. funded and supervised the study.

ACKNOWLEDGMENTS

We thank U. Schneider for animal husbandry and E. Traunecker and T. Krebs for cell sorting. This study was funded by grants to E.P. (310030-149972/1 and Synergia [SNF], Sybilla [EU FP7], and TerraIncognita [ERC]), A.K.C. (1-P01-AI091580 [NIH]), E.S.H. (R01-DK095077 [NIH]), and A.K.S. (BB/H001085/1 [BBSRC]). D.K.C. is a Wellcome Trust Career Development Fellow. A.K.S. is a Wellcome Trust Senior Investigator.

Received: April 17, 2014
Revised: July 14, 2014
Accepted: August 29, 2014
Published: October 2, 2014

REFERENCES

Artyomov, M.N., Lis, M., Devadas, S., Davis, M.M., and Chakraborty, A.K. (2010). CD4 and CD8 binding to MHC molecules primarily acts to enhance Lck delivery. Proc. Natl. Acad. Sci. USA *107*, 16916–16921.

Bridgeman, J.S., Sewell, A.K., Miles, J.J., Price, D.A., and Cole, D.K. (2012). Structural and biophysical determinants of αβ T-cell antigen recognition. Immunology *135*, 9–18.

Daniels, M.A., Teixeiro, E., Gill, J., Hausmann, B., Roubaty, D., Holmberg, K., Werlen, G., Holländer, G.A., Gascoigne, N.R., and Palmer, E. (2006). Thymic selection threshold defined by compartmentalization of Ras/MAPK signalling. Nature *444*, 724–729.

Dushek, O., Aleksic, M., Wheeler, R.J., Zhang, H., Cordoba, S.P., Peng, Y.C., Chen, J.L., Cerundolo, V., Dong, T., Coombs, D., and van der Merwe, P.A. (2011). Antigen potency and maximal efficacy reveal a mechanism of efficient T cell activation. Sci. Signal. *4*, ra39.

Dustin, M.L., Bromley, S.K., Davis, M.M., and Zhu, C. (2001). Identification of self through two-dimensional chemistry and synapses. Annu. Rev. Cell Dev. Biol. *17*, 133–157.

Ebert, P.J., Ehrlich, L.I., and Davis, M.M. (2008). Low ligand requirement for deletion and lack of synapses in positive selection enforce the gauntlet of thymic T cell maturation. Immunity *29*, 734–745.

Erman, B., Alag, A.S., Dahle, O., van Laethem, F., Sarafova, S.D., Guinter, T.I., Sharrow, S.O., Grinberg, A., Love, P.E., and Singer, A. (2006). Coreceptor signal strength regulates positive selection but does not determine CD4/CD8 lineage choice in a physiologic in vivo model. J. Immunol. *177*, 6613–6625.

Govern, C.C., Paczosa, M.K., Chakraborty, A.K., and Huseby, E.S. (2010). Fast on-rates allow short dwell time ligands to activate T cells. Proc. Natl. Acad. Sci. USA *107*, 8724–8729.

Hogquist, K.A., Jameson, S.C., Heath, W.R., Howard, J.L., Bevan, M.J., and Carbone, F.R. (1994). T cell receptor antagonist peptides induce positive selection. Cell *76*, 17–27.

Hopfield, J.J. (1974). Kinetic proofreading: a new mechanism for reducing errors in biosynthetic processes requiring high specificity. Proc. Natl. Acad. Sci. USA *71*, 4135–4139.

Huang, J., Zarnitsyna, V.I., Liu, B., Edwards, L.J., Jiang, N., Evavold, B.D., and Zhu, C. (2010). The kinetics of two-dimensional TCR and pMHC interactions determine T-cell responsiveness. Nature *464*, 932–936.

Huppa, J.B., Axmann, M., Mörtelmaier, M.A., Lillemeier, B.F., Newell, E.W., Brameshuber, M., Klein, L.O., Schütz, G.J., and Davis, M.M. (2010). TCR-peptide-MHC interactions in situ show accelerated kinetics and increased affinity. Nature *463*, 963–967.

Huseby, E.S., White, J., Crawford, F., Vass, T., Becker, D., Pinilla, C., Marrack, P., and Kappler, J.W. (2005). How the T cell repertoire becomes peptide and MHC specific. Cell *122*, 247–260.

Huseby, E.S., Crawford, F., White, J., Marrack, P., and Kappler, J.W. (2006). Interface-disrupting amino acids establish specificity between T cell receptors and complexes of major histocompatibility complex and peptide. Nat. Immunol. *7*, 1191–1199.

Jiang, N., Huang, J., Edwards, L.J., Liu, B., Zhang, Y., Beal, C.D., Evavold, B.D., and Zhu, C. (2011). Two-stage cooperative T cell receptor-peptide major histocompatibility complex-CD8 trimolecular interactions amplify antigen discrimination. Immunity *34*, 13–23.

Kerry, S.E., Buslepp, J., Cramer, L.A., Maile, R., Hensley, L.L., Nielsen, A.I., Kavathas, P., Vilen, B.J., Collins, E.J., and Frelinger, J.A. (2003). Interplay between TCR affinity and necessity of coreceptor ligation: high-affinity peptide-MHC/TCR interaction overcomes lack of CD8 engagement. J. Immunol. *171*, 4493–4503.

Kersh, G.J., Kersh, E.N., Fremont, D.H., and Allen, P.M. (1998). High- and low-potency ligands with similar affinities for the TCR: the importance of kinetics in TCR signaling. Immunity *9*, 817–826.

King, C.G., Koehli, S., Hausmann, B., Schmaler, M., Zehn, D., and Palmer, E. (2012). T cell affinity regulates asymmetric division, effector cell differentiation, and tissue pathology. Immunity *37*, 709–720.

Liu, B., Chen, W., Evavold, B.D., and Zhu, C. (2014). Accumulation of dynamic catch bonds between TCR and agonist peptide-MHC triggers T cell signaling. Cell *157*, 357–368.

McKeithan, T.W. (1995). Kinetic proofreading in T-cell receptor signal transduction. Proc. Natl. Acad. Sci. USA *92*, 5042–5046.

Melichar, H.J., Ross, J.O., Herzmark, P., Hogquist, K.A., and Robey, E.A. (2013). Distinct temporal patterns of T cell receptor signaling during positive versus negative selection in situ. Sci. Signal. *6*, ra92.

Naeher, D., Daniels, M.A., Hausmann, B., Guillaume, P., Luescher, I., and Palmer, E. (2007). A constant affinity threshold for T cell tolerance. J. Exp. Med. *204*, 2553–2559.

Nika, K., Soldani, C., Salek, M., Paster, W., Gray, A., Etzensperger, R., Fugger, L., Polzella, P., Cerundolo, V., Dushek, O., et al. (2010). Constitutively active Lck kinase in T cells drives antigen receptor signal transduction. Immunity *32*, 766–777.

O'Donoghue, G.P., Pielak, R.M., Smoligovets, A.A., Lin, J.J., and Groves, J.T. (2013). Direct single molecule measurement of TCR triggering by agonist pMHC in living primary T cells. eLife *2*, e00778.

Palmer, E., and Naeher, D. (2009). Affinity threshold for thymic selection through a T-cell receptor-co-receptor zipper. Nat. Rev. Immunol. *9*, 207–213.

Peterson, D.A., DiPaolo, R.J., Kanagawa, O., and Unanue, E.R. (1999). Cutting edge: negative selection of immature thymocytes by a few peptide-MHC complexes: differential sensitivity of immature and mature T cells. J. Immunol. *162*, 3117–3120.

Prasad, A., Zikherman, J., Das, J., Roose, J.P., Weiss, A., and Chakraborty, A.K. (2009). Origin of the sharp boundary that discriminates positive and negative selection of thymocytes. Proc. Natl. Acad. Sci. USA *106*, 528–533.

Robert, P., Aleksic, M., Dushek, O., Cerundolo, V., Bongrand, P., and van der Merwe, P.A. (2012). Kinetics and mechanics of two-dimensional interactions between T cell receptors and different activating ligands. Biophys. J. *102*, 248–257.

Schrum, A.G., Gil, D., Dopfer, E.P., Wiest, D.L., Turka, L.A., Schamel, W.W., and Palmer, E. (2007). High-sensitivity detection and quantitative analysis of native protein-protein interactions and multiprotein complexes by flow cytometry. Sci. STKE *2007*, pl2.

Smith-Garvin, J.E., Koretzky, G.A., and Jordan, M.S. (2009). T cell activation. Annu. Rev. Immunol. *27*, 591–619.

Stepanek, O., Kalina, T., Draber, P., Skopcova, T., Svojgr, K., Angelisova, P., Horejsi, V., Weiss, A., and Brdicka, T. (2011). Regulation of Src family kinases involved in T cell receptor signaling by protein-tyrosine phosphatase CD148. J. Biol. Chem. *286*, 22101–22112.

Stone, J.D., Chervin, A.S., and Kranz, D.M. (2009). T-cell receptor binding affinities and kinetics: impact on T-cell activity and specificity. Immunology *126*, 165–176.

Straus, D.B., and Weiss, A. (1992). Genetic evidence for the involvement of the lck tyrosine kinase in signal transduction through the T cell antigen receptor. Cell *70*, 585–593.

Straus, D.B., and Weiss, A. (1993). The CD3 chains of the T cell antigen receptor associate with the ZAP-70 tyrosine kinase and are tyrosine phosphorylated after receptor stimulation. J. Exp. Med. *178*, 1523–1530.

Straus, D.B., Chan, A.C., Patai, B., and Weiss, A. (1996). SH2 domain function is essential for the role of the Lck tyrosine kinase in T cell receptor signal transduction. J. Biol. Chem. *271*, 9976–9981.

Tian, S., Maile, R., Collins, E.J., and Frelinger, J.A. (2007). CD8+ T cell activation is governed by TCR-peptide/MHC affinity, not dissociation rate. J. Immunol. *179*, 2952–2960.

Valitutti, S. (2012). The Serial Engagement Model 17 Years After: From TCR Triggering to Immunotherapy. Front. Immunol. *3*, 272.

van der Merwe, P.A., and Dushek, O. (2011). Mechanisms for T cell receptor triggering. Nat. Rev. Immunol. *11*, 47–55.

Van Laethem, F., Sarafova, S.D., Park, J.H., Tai, X., Pobezinsky, L., Guinter, T.I., Adoro, S., Adams, A., Sharrow, S.O., Feigenbaum, L., and Singer, A. (2007). Deletion of CD4 and CD8 coreceptors permits generation of alphabetaT cells that recognize antigens independently of the MHC. Immunity *27*, 735–750.

Van Laethem, F., Tikhonova, A.N., Pobezinsky, L.A., Tai, X., Kimura, M.Y., Le Saout, C., Guinter, T.I., Adams, A., Sharrow, S.O., Bernhardt, G., et al. (2013). Lck availability during thymic selection determines the recognition specificity of the T cell repertoire. Cell *154*, 1326–1341.

Veillette, A., Bookman, M.A., Horak, E.M., and Bolen, J.B. (1988). The CD4 and CD8 T cell surface antigens are associated with the internal membrane tyrosine-protein kinase p56lck. Cell *55*, 301–308.

Vidal, K., Daniel, C., Hill, M., Littman, D.R., and Allen, P.M. (1999). Differential requirements for CD4 in TCR-ligand interactions. J. Immunol. *163*, 4811–4818.

Wiest, D.L., Yuan, L., Jefferson, J., Benveniste, P., Tsokos, M., Klausner, R.D., Glimcher, L.H., Samelson, L.E., and Singer, A. (1993). Regulation of T cell receptor expression in immature CD4+CD8+ thymocytes by p56lck tyrosine kinase: basis for differential signaling by CD4 and CD8 in immature thymocytes expressing both coreceptor molecules. J. Exp. Med. *178*, 1701–1712.

Williams, C.B., Engle, D.L., Kersh, G.J., Michael White, J., and Allen, P.M. (1999). A kinetic threshold between negative and positive selection based on the longevity of the T cell receptor-ligand complex. J. Exp. Med. *189*, 1531–1544.

Yamagata, T., Mathis, D., and Benoist, C. (2004). Self-reactivity in thymic double-positive cells commits cells to a CD8 alpha alpha lineage with characteristics of innate immune cells. Nat. Immunol. *5*, 597–605.

Yin, L., Dai, S., Clayton, G., Gao, W., Wang, Y., Kappler, J., and Marrack, P. (2013). Recognition of self and altered self by T cells in autoimmunity and allergy. Protein Cell *4*, 8–16.